

Digital holographic microscopy: a noninvasive contrast imaging technique allowing quantitative visualization of living cells with subwavelength axial accuracy

Pierre Marquet, Benjamin Rappaz, and Pierre J. Magistretti

Department of Physiology, University of Lausanne, CH-1005 Lausanne, Switzerland

Etienne Cuche and Yves Emery

Lyncée Tec SA, Rue du Bugnon 7, CH-1005 Lausanne, Switzerland

Tristan Colomb and Christian Depeursinge

Ecole Polytechnique Fédérale de Lausanne, Laboratoire d'Optique Appliquée, CH-1015 Lausanne, Switzerland

Received June 25, 2004

We have developed a digital holographic microscope (DHM), in a transmission mode, especially dedicated to the quantitative visualization of phase objects such as living cells. The method is based on an original numerical algorithm presented in detail elsewhere [Cuche *et al.*, *Appl. Opt.* **38**, 6994 (1999)]. DHM images of living cells in culture are shown for what is to our knowledge the first time. They represent the distribution of the optical path length over the cell, which has been measured with subwavelength accuracy. These DHM images are compared with those obtained by use of the widely used phase contrast and Nomarski differential interference contrast techniques. © 2005 Optical Society of America

OCIS codes: 090.0090, 090.1000, 110.1650, 100.2000, 170.1650.

In biology, most microscopy specimens, in particular living cells, are transparent and differ only slightly from their surroundings in terms of absorbance and color, thus providing a modest change in the amplitude of the light wave. Examination of such transparent specimens, which have the capacity to alter the phase of the detected light wave and are called phase objects, has led to the development of optical contrast-enhancing imaging techniques.

Among the numerous modalities of contrast-enhancing techniques that have been developed for visualization of noninvasively unstained transparent specimens, phase contrast (PhC), initially proposed by Zernike as a means of image contrast,^{1,2} as well as Nomarski's differential interference contrast³ (DIC) are available for high-resolution light microscopy⁴ and are widely used in biology. Briefly, these two contrast techniques allow one to transform phase information into amplitude or intensity modulation, which can be detected by photosensitive media.

In addition to the above-mentioned microscopy techniques, the availability of lasers, modulators, and sophisticated detectors (in many cases CCD cameras) have promoted the development of various interferometric techniques. Unlike the PhC and DIC microscopy techniques, interferometric techniques present the great advantage of yielding quantitative measurements of parameters, including the phase distribution produced by transparent specimens. However, whereas interferometric techniques are widely used in metrology, only a few applications have been reported in biology.^{4–7} This is probably due to the fact that interferometric measuring setups often

involve complex laser systems, including modulators and piezo-driven mirrors, requiring complex handling.

In this Letter we present an interferometric technique based on a digital holography principle that allows one to measure the phase or the optical path length distribution created by living cells. The digital holographic microscope (DHM) that we have developed provides a simplified and easy-to-operate technique compared with classical interferometry. Indeed, digital holography, i.e., digital recording and numerical reconstruction of holograms, offers new perspectives in imaging, because numerical processing of a complex wave front allows one to compute simultaneously the intensity and the phase distribution⁸ of the propagated wave. In optical microscopy, digital holography^{9–11} has made it possible to focus numerically on different object planes without using any optomechanical movement.^{10,12} Moreover, different lens aberrations^{10,13} can be corrected by a numerical procedure. In this Letter, and for the first time to our knowledge, absolute phase distribution images of living neurons in a culture obtained by use of a DHM with an accuracy in the 2–4° range are presented. To evaluate the DHM compared with the standard and widely used techniques of PhC and DIC microscopy in biology, images of living neurons obtained with PhC, DIC, and the DHM are presented.

The DHM is basically a Mach–Zehnder interferometer (Fig. 1). A laser beam is divided by a beam splitter (BS). The sample (S) is illuminated by one beam through a condenser (C). A microscope objective (MO) collects the transmitted light and forms the object wave (O), which interferes, in an off-axis geometry,

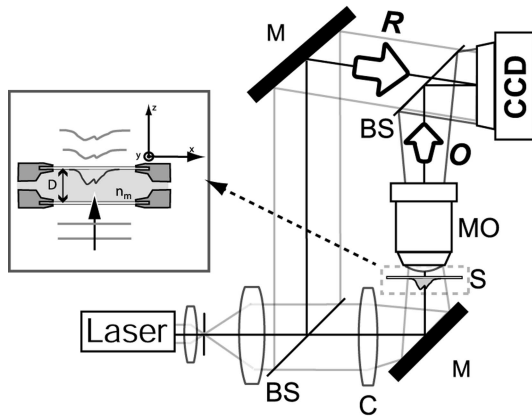


Fig. 1. Basic configuration of the DHM. Inset, schematic representation of cultured cells mounted in a closed perfusion chamber. M, mirror. Other abbreviations defined in text.

with a reference wave **R** to produce hologram intensity. The DHM method was developed with standard commercial optomechanical components. A linearly polarized helium–neon laser (10 mW, $\lambda = 633$ nm) was used as a coherent light source. Neurons were observed through a $60\times$, 0.8-N.A. microscope objective that permitted diffraction-limited transverse resolution of ~ 0.6 μm (Ref. 10) and a full field of view of 120 $\mu\text{m} \times 120$ μm . Holograms (8 bits, 512×512 pixels) were recorded on a standard monochrome CCD video camera (PCO VX44-C). Acquisition, digitization, and reconstruction of holograms were performed with a 2.66-MHz Pentium IV computer using a video frame grabber (IMAQ-PCI) in the LabVIEW environment (National Instruments). The measured irradiance at the neuronal plane was ~ 200 $\mu\text{W}/\text{cm}^2$, which is several orders of magnitude lower than the power used in a classical confocal laser scanning microscope.

Quantitative phase images are obtained by the DHM (Fig. 2C) according to an original procedure using a single recorded hologram.¹⁴ The value of each pixel i of the reconstructed phase image can be expressed as

$$\begin{aligned} \varphi_i &= \frac{2\pi}{\lambda} \int_0^{d_i} n_{c,i}(z) dz + n_m(D - d_i) \\ &= \frac{2\pi}{\lambda} [(\bar{n}_{c,i} - n_m)d_i + n_m D], \end{aligned} \quad (1)$$

where λ is the wavelength, z is the axial coordinate, d_i is the cellular thickness corresponding to pixel i , $n_{c,i}(z)$ is a function representing the value of the intracellular refractive index along cellular thickness d_i , $\bar{n}_{c,i} = (1/d_i) \int_0^{d_i} n_{c,i}(z) dz$ is the intracellular mean refractive index ($\bar{n}_{c,i}$) along cellular thickness d_i , n_m is the constant refractive index of the surrounding medium, and D is the thickness of the flow chamber (inset of Fig. 1). Product $n_m D$ is a reference value that can be measured anywhere in the vicinity of the cell. Monitoring this reference value is important because it permits compensation for the mechanical and the thermal instabilities of the setup during the experiment.

The dark PhC and transmitted DIC images (shearing mode) presented in this Letter were obtained from the stage of a microscope (Zeiss Axiovert 135M) equipped with a CCD camera, and the neurons were observed through a $63\times$, 1.25-N.A. oil-immersion microscope objective (Zeiss plan Neofluar). Primary cultures of mouse cortical neurons were prepared according to the technique presented by Brewer *et al.*¹⁵

Images of the same living neurons in culture obtained with a DHM and PhC, and DIC microscopy are presented in Fig. 2. For each pixel i , the component of the signal that accounts for the cell-specific contribution to the optical path length $(\bar{n}_{c,i} - n_m)d_i$ [Eq. (1)], depends on the cell thickness (d_i), the intracellular mean refractive index ($\bar{n}_{c,i}$), and the refractive index of the perfusion solution (n_m), whose value $n_m = 1.3336 \pm 0.0002$ was measured with an Abbe refractometer at $\lambda = 633$ nm. By assuming, in the first approximation, a constant and homogeneous cellular refractive index $n_c = 1.375$,^{7,16} one can estimate that a phase shift of 10° corresponds to a cellular thickness of ~ 0.45 μm . This translates to a thickness of 1–3 μm for the neuronal processes and ~ 8 –10 μm for the cell body and allows a three-dimensional representation of living neurons (Fig. 2D). With the

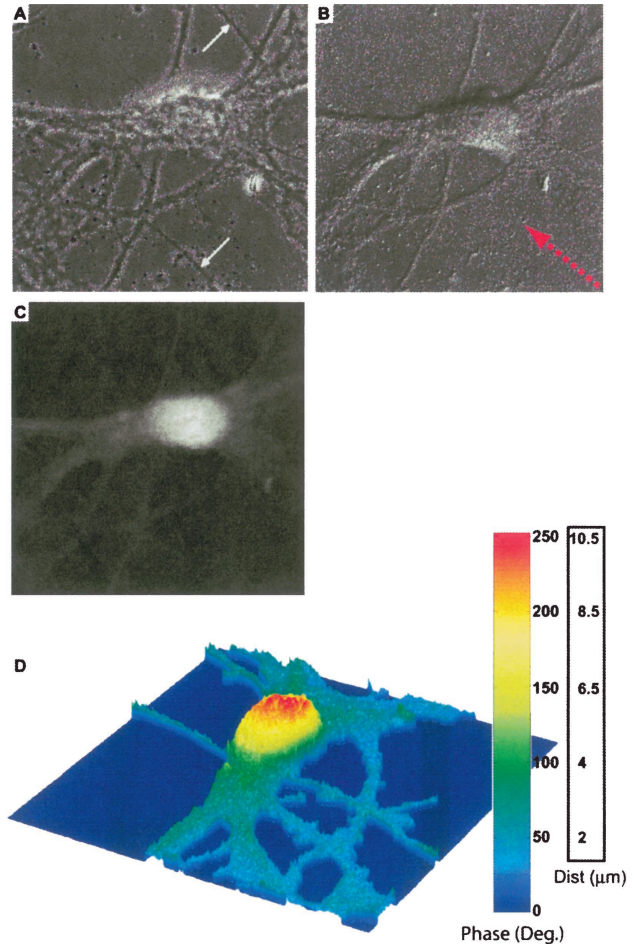


Fig. 2. Images of a living mouse cortical neuron in culture: A, dark PhC image; B, DIC image; C, raw image; D, perspective image in false colors of the phase distribution obtained with the DHM.

assumption of a constant intracellular refractive index (which can be discussed given a certain degree of heterogeneity of the constituents), these estimates of cell morphology give realistic values of typical neuron dimensions. Using the same assumption for the refractive index, and based on a phase measurement accuracy of $2\text{--}4^\circ$, we obtain a cellular axial (or vertical) accuracy of $\sim 160\text{--}320$ nm.

Comparatively, images of the same neuron obtained with PhC and DIC microscopy are presented. The dark PhC image (Fig. 2A) makes the neuronal processes particularly visible. However, PhC suffers from well-known optical artifacts, namely, the halo and shading off,⁴ that complicate the correct interpretation of PhC images in terms of optical path length. In these dark phase contrast images (Fig. 2A) a halo is seen in the background as a bright zone surrounding the neuronal body and processes. The shading-off effect generates a phase increase in the central part of the neuronal body, making it appear brighter than the thin neuronal processes.

The predominant feature of DIC images (Fig. 2B) is their three-dimensional appearance as a result of virtual lateral illumination, or the shadow-cast effect. This effect results from both the spatial directional gradient along the shear angle of the intracellular refractive index and from the cellular thickness. The contrast of DIC images is, therefore, not symmetrical and varies proportionally to the cosine of the angle made by the azimuth of the object and the direction of wave-front shear. Consequently, the contrast of structures, whose phase-shift gradient is approaching the direction perpendicular to that of the wave-front shear, becomes progressively less marked and eventually disappears. This is typically the case for neuronal processes parallel to the wave-front shear direction (red arrow, Fig. 2B), which are not actually visible in the DIC image (Fig. 2B) and are indicated by white arrows in the PhC image (Fig. 2A). However, there have been attempts, requiring complex procedures, to overcome this drawback and to make possible the reconstruction of the optical path-length distributions from DIC images.¹⁷ On the other hand, unlike PhC images, DIC images do not suffer from the halo effect, which can make some structures and minute details invisible.

Finally, it should be mentioned that the quantitative phase distribution images obtained by the DHM are less than the DIC and PhC images, making the visualization of some fine neuronal processes difficult. Although the microscope objective used for the DHM has a lower N.A. (0.8) than those of the DIC and PhC microscope objectives (N.A. 1.25), this loss of sharpness results mainly from the presence of coherent noise originating from different sources such as dust particles, scratches, and defects on and in the optical elements, in particular stray reflections. This coherent noise results in a temporally stable granular structure, whose phase amplitude measured on blank images is approximately $2\text{--}4^\circ$. However, as can be observed from Fig. 2D, image processing allows a 3D perspective representative of living neurons and makes most of the neuronal processes clearly visible. Moreover, the DHM can be used with low-coherence

light sources,¹² allowing one to reduce the coherent noise.

In summary, we have demonstrated that a DHM is an efficient and easy-to-operate interferometric technique that can be used in a biological environment as a noninvasive phase contrast microscope to visualize transparent objects such as living cells in a culture. This simplified interferometric technique presents several appealing advantages. In particular, digital hologram processing, which allows the restoration and the reshaping of a complex wave front, provides the capability of replacing complex optical adjustment procedures by simple numerical steps. This is particularly well illustrated by the digital correction of the wave-front deformation induced by the microscope objective, which eliminates the introduction, in the reference arm, of a second identical microscope objective that must be aligned with high precision. Moreover, unlike in PhC and DIC microscopy, the DHM provides the quantitative distribution of the optical path length created by transparent specimens. This quantitative distribution contains information concerning both morphology and refractive index of the observed specimen. In addition, the high sensitivity of these phase-shift measurements allows one to achieve subwavelength axial accuracy. As far as living cells in culture are concerned this corresponds to an axial accuracy in the range of $160\text{--}320$ nm, offering attractive possibilities for the visualization of the cellular dynamics.

This work was supported by grants 31-51882.97, 21-67068.01, and 205320-103885/1 from the Swiss National Science Foundation. P. Marquet's e-mail address is pierre.marquet@unil.ch.

References

1. F. Zernike, *Physica* **9**, 686 (1942).
2. F. Zernike, *Physica* **9**, 974 (1942).
3. G. Nomarski, *J. Phys. Radium* **16**, 9 (1955).
4. M. Pluta, *Advanced Light Microscopy* (Elsevier, New York, 1988), Vol. 2.
5. R. Pawluczyk, *Appl. Opt.* **28**, 3871 (1989).
6. G. A. Dunn and D. Zicha, *J. Cell Sci.* **108**, 1239 (1995).
7. J. Farinas and A. S. Verkman, *Biophys. J.* **71**, 3511 (1996).
8. U. Schnars and W. P. O. Jüptner, *Meas. Sci. Technol.* **13**, R85 (2002).
9. T. Zhang and I. Yamaguchi, *Opt. Lett.* **23**, 1121 (1998).
10. E. Cuche, P. Marquet, and C. Depeursinge, *Appl. Opt.* **38**, 6994 (1999).
11. G. Indebetouw and P. Klysubun, *J. Opt. Soc. Am. A* **18**, 319 (2001).
12. F. Dubois, L. Joannes, and J.-C. Legros, *Appl. Opt.* **38**, 7085 (1999).
13. A. Stadelmaier and J. H. Massig, *Opt. Lett.* **25**, 1630 (2000).
14. E. Cuche, F. Bevilacqua, and C. Depeursinge, *Opt. Lett.* **24**, 291 (1999).
15. G. J. Brewer, J. R. Torricelli, E. K. Evege, and P. J. Price, *J. Neurosci. Res.* **35**, 567 (1993).
16. A. Dunn and R. Richards-Kortum, *IEEE J. Select. Top. Quant. Electron.* **2**, 898 (1996).
17. E. B. Van Munster, L. J. Van Vliet, and J. A. Aten, *J. Microsc. (Oxford)* **188**, 149 (1997).